Geophysical Journal International

Geophys. J. Int. (2019) **218,** 755–761
Advance Access publication 2019 April 20
GJI Gravity, Geodesy and Tides

doi: 10.1093/gji/ggz187

Surface displacements of Aso volcano after the 2016 Kumamoto earthquake based on SAR interferometry: implications for dynamic triggering of earthquake–volcano interactions

Wataru Yamada,[1] Kazuya Ishitsuka,[2] Toru Mogi[3] and Mitsuru Utsugi[4]

[1]*Cooperative Program for Resources Engineering, Graduate School of Engineering, Hokkaido University, Sapporo 060-8628, Japan. E-mail: mayusuk1@eis.hokudai.ac.jp*
[2]*Department of Urban Management, Graduate School of Engineering, Kyoto University, Yoshida-honmachi, Sakyo-ku, Kyoto 606-8501, Japan*
[3]*Division of Sustainable Resources Engineering, Graduate School of Engineering, Hokkaido University, N13W8, Sapporo 060-8628, Japan*
[4]*Aso Volcanological Laboratory, Institute for Geothermal Sciences, Graduate School of Science, Kyoto University, Yoshida-honmachi, Sakyo-ku, Kyoto 606-8501, Japan*

Accepted 2019 April 19. Received 2019 April 5; in original form 2018 August 12

SUMMARY

The 2016 Kumamoto earthquake involved a series of events culminating in an M_w 7.0 main shock on 2016 April 16; the main-shock fault terminated in the caldera of Aso volcano. In this study, we estimated surface displacements after the 2016 Kumamoto earthquake using synthetic aperture radar interferometry analysis of 16 Phased Array Type L-band Synthetic Aperture Radar-2 images acquired from 2016 April 18 to 2017 June 12 and compared them with four images acquired before the earthquake. Ground subsidence of about 8 cm was observed within about a 3 km radius in the northwestern part of Aso caldera. Because this displacement was not seen in data acquired before the 2016 Kumamoto earthquake, we attribute this displacement to the 2016 Kumamoto earthquake. Furthermore, to estimate the source depth of the surface displacement, we applied the Markov chain Monte Carlo method to a spherical source model and obtained a source depth of about 4.8 km. This depth and position are nearly in agreement with the top of a low-resistivity area previously inferred from magnetotelluric data; this area is thought to represent a deep hydrothermal reservoir. We concluded that this displacement is due to the migration of magma or aqueous fluids.

Key words: Japan; Satellite geodesy; Interferometry; Calderas; Volcano monitoring.

1 INTRODUCTION

Large earthquakes change the stress state, fracture zone form and permeability of the crust. They may also change the mechanical state of a magma chamber and its surrounding area, influencing volcanic unrest and eruption. Hill *et al.* (2002) reviewed the mechanisms of earthquake-induced volcanic activities: (i) static stress changes caused by crustal deformation, (ii) quasi-static stress changes associated with viscoelastic relaxation of the lower crust and upper mantle and (iii) dynamic stresses induced by seismic vibration. As examples, the sequence of the eruption after the Cascadia earthquake (M_w 8.7–9.2) of 1700 has been considered to have been caused by static stress changes, and the unrest of the Long Valley caldera in eastern California associated with the 1992 Landers earthquake was attributed to both static stress changes and dynamic triggering (Hill *et al.* 2002). Similarly, in hydrothermal systems, groundwater level changes have frequently been observed after large earthquakes and interpreted as the cumulative influences of these effects (Manga *et al.* 2012).

Surface displacement measurements have provided important clues to understand the mechanical disturbances around volcanoes and groundwater systems associated with earthquakes. For example, Takada & Fukushima (2013) showed that volcanic areas of the Tohoku region subsided by as much as 5−15 cm during the 2011 Tohoku earthquake (M_w 9.0) because of extensional stress around magma chambers. Poroelastic displacements due to groundwater migration were inferred by Peltzer *et al.* (1998) and Fialko (2004) following the 1992 Landers earthquake, and by Jonsson *et al.* (2003) following the 2000 Iceland earthquake. Ishitsuka *et al.* (2017) showed ground uplift related to permeability enhancement after the 2011 Tohoku earthquake. However, such examples are still limited, and further observations are desirable to clarify the influence of large earthquakes on volcanoes and hydrothermal systems.

Aso volcano, which is located in the central part of Kyushu island, Japan, comprises a caldera that extends about 18 km in the east–west direction and about 25 km in the north–south direction (Fig. 1). The caldera was formed by four large eruptions that occurred about 300 000–90 000 yr ago; currently, related volcanic activity continues unabated. In particular, Nakadake crater has been active during

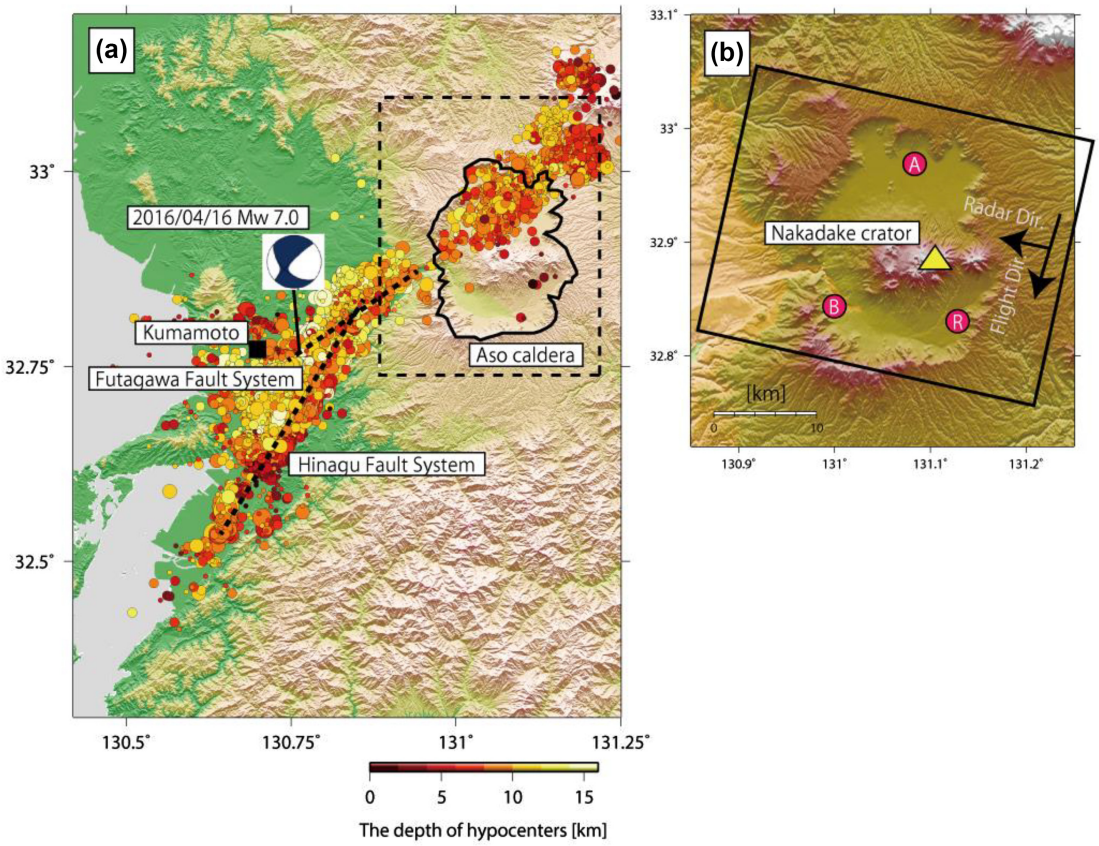

Figure 1. (a) Hypocentres associated with the 2016 Kumamoto earthquake, 2016 April 14−30. The dashed lines approximately indicate the Futagawa and Hinagu fault systems, and the dashed rectangle is the area of (b). The focal sphere for the main shock was derived by F-net managed by the National Research Institute for Earth Science and Disaster Resilience (Asano & Iwata 2016). (b) Area of interest in this study (the black rectangle). A, B and R mark the locations of the GEONET stations Aso, Chouyou and Takamori, respectively. R indicates the reference GEONET station.

the past 70 yr, producing several Strombolian eruptions. The 2016 Kumamoto earthquake ruptured the Futagawa and Hinagu fault systems in Kyushu island (Fig. 1). The main shock of the 2016 Kumamoto earthquake occurred with M_w 7.0 on 2016 April 16 at 15 km width and 40 km length along the Futagawa fault system (Fig. 1). Recent research showed that changes in stress would have occurred in Aso volcano as well as the surrounding aquifers due to the 2016 Kumamoto earthquake (e.g. Yagi *et al.* 2016). Yagi *et al.* (2016) found that the edge of the fault slip terminated in the northwestern part of Aso caldera by estimating the fault slip distribution using teleseismic body waves, which implies that the fault rupture stopped near the high-temperature area around the magma chamber. These previous studies suggest that the hydrothermal or magma system at Aso volcano was influenced by the 2016 Kumamoto earthquake.

In this study, to understand the mechanical influences of the 2016 Kumamoto earthquake on Aso volcano, we estimated surface displacements about 1 yr and 2 months after the earthquake using synthetic aperture radar interferometry (InSAR) (Massonnet & Feigl 1998) and compared the results with those from before the 2016 Kumamoto earthquake. Moreover, we estimated the position and size of the pressure source that caused the surface displacements in Aso caldera using the Mogi model (Mogi 1958).

2 DATA AND METHOD

The area of interest is a 40 km × 30 km area that includes Aso caldera (Fig. 1). We used 20 images taken on a descending orbit between 2015 February 9 and 2017 June 12 (Table 1) by the Phased Array Type L-band Synthetic Aperture Radar-2 (PALSAR-2) instrument aboard the Advanced Land Observing Satellite-2 (ALOS-2). Four of them were acquired before the 2016 Kumamoto earthquake, and 16 were acquired afterwards (Table 1). Interferometric pairs from before the 2016 earthquake were created between data sets with the shortest temporal baseline, whereas interferometric pairs after the 2016 earthquake were created with respect to data acquired on 2016 April 18, 2 d after the main shock. To compensate for topographic effects and geocoding, we used a 10 m mesh digital elevation model (DEM) provided by the Geospatial Information Authority of Japan. For conducting InSAR analysis, we used the Radar Interferometry Calculation Tool (Ozawa *et al.* 2016).

We first applied a multilook procedure with factors of 5 each in the azimuth and range directions at the interferogram generation step. We then simulated the orbital and topographic phases using DEM and precise orbital data and subtracted them from the initial interferograms. In addition, to remove random noise, we applied adaptive filtering. For phase unwrapping, we applied the minimum cost flow algorithm using SNAPHU (Chen & Zebker 2000). The atmospheric delay components correlated with topography were removed by a best-fitting linear function in a least-squares sense. Finally, we applied geocoding to obtain surface displacements in longitude–latitude coordinates from those in range–azimuth coordinates.

We then modelled the estimated surface displacement by assuming a spherical deformation source lying directly beneath the

Table 1. SAR data used in this study.

Data before the 2016 earthquake		Data after the 2016 earthquake			
Date	Bperp (m)	Date	Bperp (m)	Date	Bperp (m)
2015/02/09	0	2016/04/18	0	2016/09/05	−82.6
2015/02/23	−57.6	2016/05/02	88.5	2016/09/19	−147.3
2015/09/07	−145.4	2016/05/16	247.7	2016/10/03	−142.8
2016/03/07	−15.2	2016/06/13	−40.3	2016/10/17	−147.7
–	–	2016/06/27	181.0	2016/10/31	−171.6
–	–	2016/07/11	20.1	2016/11/14	−164.5
–	–	2016/07/25	33.2	2017/03/06	187.4
–	–	2016/08/08	−7.2	2017/06/12	26.5

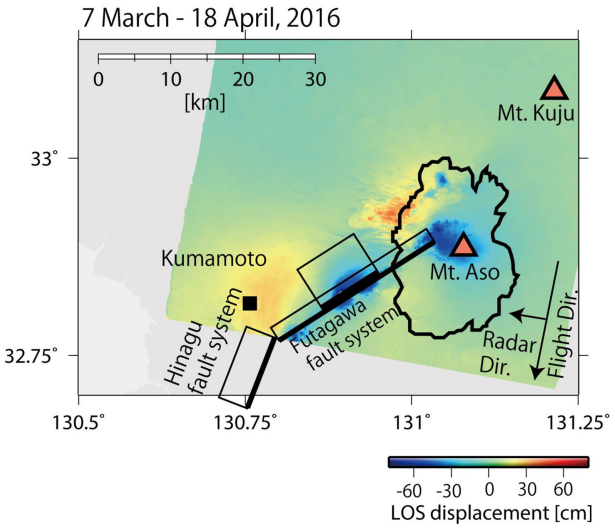

Figure 2. Surface coseismic displacement during 2016 March 7 and April 18. The foreshock and main shock of 2016 Kumamoto earthquake occurred on 14 April and 16 April, respectively. The black rectangles are ruptured fault traces associated with the 2016 Kumamoto earthquake (based on Himematsu & Furuya 2016).

deformed ground and applying the homogeneous and isotropic elastic body model proposed by Mogi (1958). This model uses four parameters to simulate surface displacement: 3-D source position, and amount of volume change. We applied the Markov chain Monte Carlo (MCMC) method for estimating the model parameters (Aster *et al.* 2013). The MCMC method samples the model space in such a way that the density of the points eventually becomes proportional to the probability density function of the model parameters. Circular subsampling was conducted such that the density of estimated surface displacement became smaller at areas farther from the centre of the displacement. For the shear modulus, Poisson's ratio and the number of iterations, we used the values of 20 GPa, 0.25 and 100 000, respectively.

3 RESULTS

3.1 InSAR analyses

In the interferometric pair that includes the main shock (2016 March 7−April 18), we detected displacement of about 50−60 cm away from the satellite at the northwest side of the caldera, and displacement of about 60 cm towards the satellite around the northwest flank of Aso volcano (Fig. 2). In the ALOS-2/PALSAR-2 data acquired before the 2016 Kumamoto earthquake, remarkable ground displacement was detected only within about 500 m of Nakadake crater (Fig. 3a).

From the interferometric results after the 2016 earthquake, we found that displacement away from the satellite, which can be regarded as subsidence, occurred in an area about 6−7 km northwest from Nakadake crater. This displacement occurred along the fault soon after the earthquake (interferometric pairs of 2016 April 18−May 2 and April 18−May 16; Fig. 3b). In contrast, in the pair for 2016 April 18−June 13 and pairs from later acquisitions, the subsidence formed a circular shape (Fig. 3b). The subsidence increased over time, finally reaching a displacement of about 8 cm in a circular area with a diameter of about 6−8 km during the 14 months after the earthquake (2016 April 18−2017 June 12; Figs 3b and c).

At Nakadake crater, local surface displacement occurred within about a 500 m diameter in the crater (Fig. 3b). This displacement occurred in directions both towards and away from the satellite at various times. A small phreatomagmatic eruption occurred in the crater on 2016 October 8 (JMA 2016). In the interferometric pair that covers that period, we detected interferometric decorrelation likely associated with changes in the surface covering near the crater, whereas significant surface displacement was not found. Thus, the phreatomagmatic eruption did not significantly change the volumes of hydrothermal reservoirs or the magma chamber.

To validate our InSAR results, we compared them with Global Navigation Satellite System (GNSS) data. We used the GNSS daily coordinate values (F3 solution) of GEONET, managed by the Geospatial Information Authority of Japan. We used three GEONET stations: Chouyou (station 960701), Aso (960703) and Takamori (960704) within Aso caldera (Fig. 1b). To reduce random noise, we used the average values over 11 d, including 5 d before and after the SAR acquisitions. The data for 2016 April 18, for which we used the average value over 5 d, were an exception due to its proximity to the earthquake date. We set Takamori as the reference station and obtained the relative displacement at the other two GNSS points. The results of the comparison yielded root-mean-square errors (RMSEs) of 0.8605 cm (Aso) and 0.7401 cm (Chouyou), which are within the typical range for InSAR analysis of ALOS-2/PALSAR-2 data (Nishiguchi *et al.* 2017).

3.2 Estimation of surface displacement source

For modelling the displacement source, we used the interferometric pair of 2016 April 18−October 17 because, compared with other pairs, it had a larger signal-to-noise ratio and sufficiently long temporal span. We regarded the deformation source with the smallest RMSE as optimal. Fig. 4 shows the InSAR results, modelled surface displacement, and residual image (difference between observed and

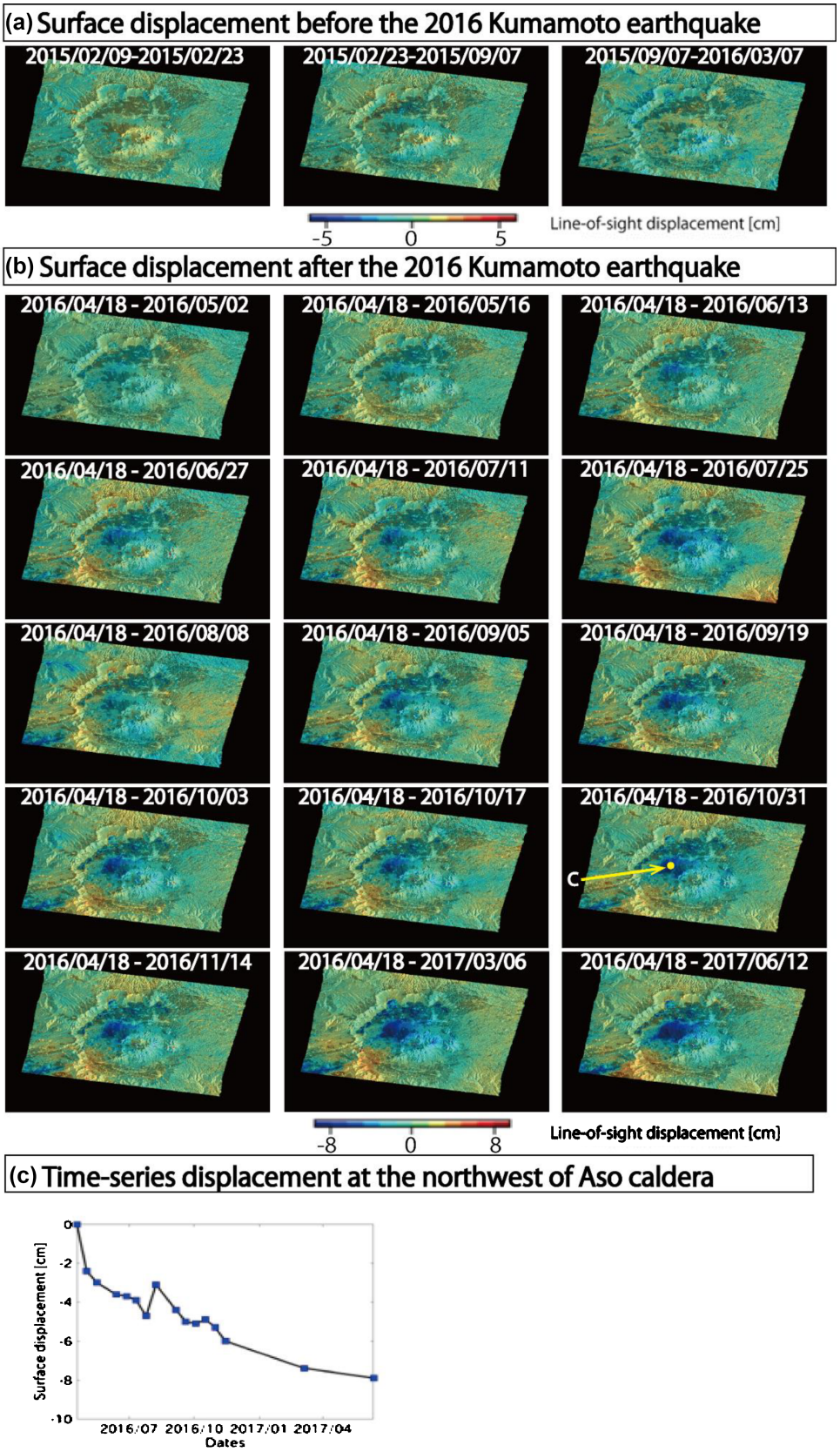

Figure 3. Line-of-sight displacement maps derived from InSAR analysis. (a) Surface displacement maps before the 2016 Kumamoto earthquake; (b) surface displacement maps after the earthquake; (c) time-series surface displacement northwest of Aso caldera [‘c’ in panel (b)].

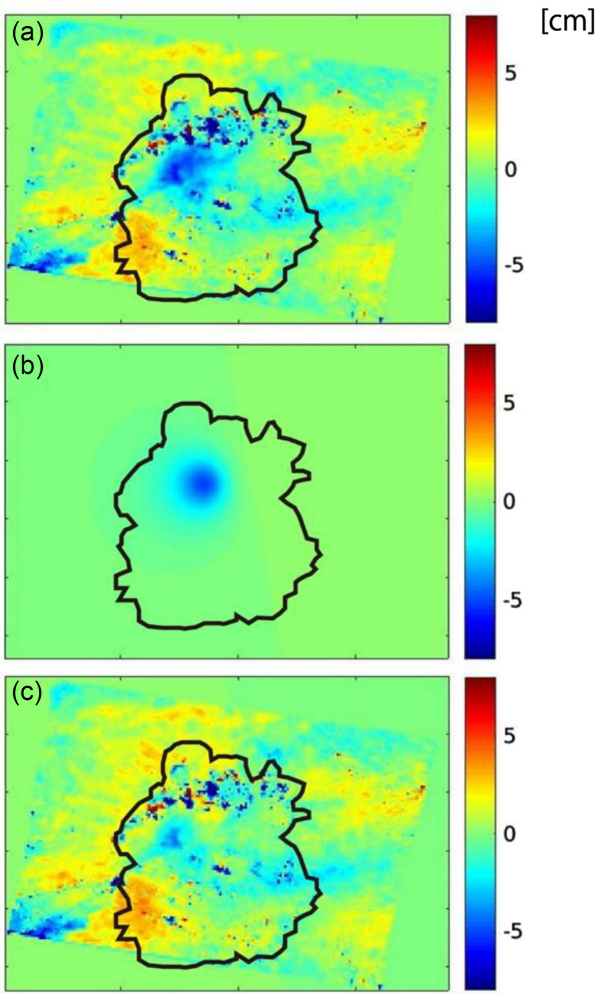

Figure 4. (a) Line-of-sight surface displacement of the interferometric pair of 2016 April 18−October 17; (b) estimated surface displacement by optimal deformation source; (c) difference between (a) and (b) (residual image).

modelled displacement). The optimal model has a depth of about 4.8 km. Because displacement away from the satellite in the northwestern part of the caldera is largely eliminated in the residual image, we concluded that the optimum model is reasonable.

4 DISCUSSIONS

This study found local ground subsidence in the northwest part of Aso caldera after the 2016 Kumamoto earthquake. Previously, Nobile *et al.* (2017) estimated the annual surface displacements from 1996 to 2010 using InSAR analysis, and Sudo *et al.* (2006) evaluated the results of levelling in the region southwest of Nakadake crater between 1932 and 2004. Notable subsidence was not reported around the northwest caldera. Therefore, we conclude that the local subsidence in the northwest Aso caldera detected in this study is associated with the 2016 Kumamoto earthquake.

Hata *et al.* (2016, 2018) estimated the 3-D resistivity structure around Aso caldera using magnetotellurics and found three low-resistivity areas identified as a magma chamber and hydrothermal systems. One was at a depth of 4−8 km about 2−3 km west of Nakadake crater, and another was roughly consistent with the range of the magma chamber estimated by Sudo *et al.* (2006). Furthermore, Hata *et al.* (2016, 2018) showed that a third low-resistivity region also existed about 6−20 km deep and about 5−6 km northwest of Nakadake crater. We concluded that this low resistivity is associated with magma or hydrothermal fluid. The 3-D location of the displacement source estimated in this study corresponds to the top of this deep low-resistivity region but not with the location of the well-known magma chamber. The source position implies that a deep hydrothermal reservoir or magma chamber was influenced by the 2016 Kumamoto earthquake.

It has been shown that the estimated source depth depends on both the heterogeneity of subsurface structures and source geometry (Dieterich 1975; Fialko *et al.* 2001; Masterlark 2007; Masterlark *et al.* 2016). Dieterich (1975) and Fialko *et al.* (2001) showed that estimating a source depth by the Mogi model only from 1-D displacement produces a shallower source when the true geometry is a sill shape, and a deeper source when the geometry is a dyke shape. On the other hand, regarding the heterogeneity, Masterlark (2007) and Masterlark *et al.* (2016) showed that soft crust with small elastic modulus, which is typical in calderas, amplifies the magnitude of surface displacement. Given this caldera structure, the pressure source modelled as a homogeneous elastic body has an estimated depth shallower than the actual source depth. In Masterlark (2007), when weak material was above the pressure source at Okmok volcano, Alaska, the estimated source depth was 1200–1400 m shallower compared with an estimated depth based on homogeneous elastic half-space as in Mogi (1958). Although the subsurface structure of Aso caldera has not been clarified, the density structure from gravity measurements (Miyakawa *et al.* 2016) and seismic wave structure from well-recorded earthquakes (Sudo & Kong 2001) implies weak materials beneath Aso. Therefore, the actual pressure source may be deeper than the depth estimated by the Mogi model in our study. Thus, our interpretation is that the source was within the deep low-resistivity region by Hata *et al.* (2016, 2018).

Here, we discuss the three mechanisms proposed for associating volcanic activity and large earthquakes (Section 1, Hill *et al.* 2002), which are static stress changes, viscoelastic relaxation and dynamic triggering. The fault motion of the 2016 Kumamoto earthquake (Yagi *et al.* 2016) induced shear stresses in the local deformation area. Theoretical estimation of surface displacements due to pore pressure transients, which could be induced by the static stress changes, did not show a significant subsidence pattern west of Aso caldera. In addition, most previous studies showed that post-seismic pore pressure transients occur within a few months, which is much shorter than our observation interval (e.g. Jonsson *et al.* 2003). Therefore, static stress changes cannot explain the local subsidence pattern at Aso.

The likelihood of viscoelastic relaxation is also low. Although brittle−ductile transition beneath the volcano occurs about 5 km deep (Yagi *et al.* 2016), the ductile body is widely distributed (i.e. 5−20 km deep), and the transition beneath Nakadake crater would be shallower than the local subsidence area due to ongoing volcanic activity. Therefore, viscoelastic relaxation is unlikely to generate local displacement only northwest of the caldera with spatial dimensions of about 6 km × 6 km. Ohzono *et al.* (2012) showed that viscoelastic relaxation caused surface displacements after the 2008 Iwate–Miyagi Nairiku earthquake with a spatial wavelength of about 20−50 km, despite the presence of high heat gradients. Thus, viscoelastic relaxation would occur at a wider spatial scale even around a volcanic zone.

These geological inferences lead us to conclude that dynamic triggering was the most likely cause of the local surface displacement in the northwestern part of the caldera. Two major mechanisms of dynamic triggering are (i) relaxation of the magma body and (ii)

hydraulic surge. Currently, we cannot rule out either of these two possibilities. In magma body relaxation, the magma chamber is considered to exist in a partially crystallized state, which is disrupted by strong seismic vibration, releasing any accumulated stress differences. The deformation at the Long Valley caldera following the 1992 Landers earthquake is interpreted as a result of this process (Hill *et al.* 2002). Because the temporal deformation pattern of magma relaxation evolves exponentially as a function of time, this pattern can explain our observations. This would mean that the magma body moved downwards. In contrast, the hydraulic surge mechanism assumes an impermeable seal between the plastic crust and magma body and that the hydrothermal system originates from a slab that exists beneath the impermeable zone. If the impermeable zone is broken by strong vibration or faulting, trapped hydrothermal fluid migrates and deformation occurs. Such a deep hydrothermal system is typical in supercritical geothermal systems (e.g. Reinsch *et al.* 2017). If hydraulic surge occurred at Aso, this suggests the presence of deep supercritical fluids beneath the northwest part of the caldera. This mechanism is thought to induce surface displacement, but surface displacement by this phenomenon has not actually been observed as far as we know. We consider this mechanism to be possible for Aso because groundwater level changes were observed around the volcano: they increased by as much as about 3−6 m at the western flank of Aso volcano for about 1 yr after the 2016 Kumamoto earthquake (Kagabu *et al.* 2018). This increase may be associated with the release of deep groundwater under the volcano, which was previously estimated for an adjacent mountain after the 1999 Chi-Chi earthquake (Wang *et al.* 2004). Therefore, the release of deep groundwater might have induced the surface displacement in the northwest Aso caldera.

5 CONCLUSIONS

We carried out InSAR analysis using 20 observations by ALOS-2/PALSAR-2 between 2015 February 9 and 2017 June 12 to detect surface displacement at Aso volcano before and after the 2016 Kumamoto earthquake. In particular, we found that ground subsidence in an area of about 6 km × 6 km occurred over 1.3 yr in the northwest Aso caldera. Because this displacement pattern was not found in data acquired before the 2016 Kumamoto earthquake, we concluded that most of the observed displacement occurred due to the influence of the 2016 Kumamoto earthquake. Modelling of the local surface displacement estimated the depth of the displacement source to be about 4.8 km. The spatial position of this pressure source corresponds to the top of the low-resistivity region detected by Hata *et al.* (2016, 2018), which is regarded as high-pressure fluid. Therefore, the displacement was likely due to the movement of magma or high-pressure hydrothermal fluid.

ACKNOWLEDGEMENTS

5 Acknowledgements

ALOS-2/PALSAR-2 level 1.1 data were provided by the PALSAR Interferometry Consortium to Study our Evolving Land Surface in cooperation with the Earthquake Research Institute, University of Tokyo. A part of ALOS-2/PALSAR-2 data used in this study were provided through the 1st research announcement of the earth observations by the Japan Aerospace Exprolation Agency. The ALOS-2/PALSAR-2 data belong to the Japan Aerospace Exploration Agency. The hypocentre data were provided by the National Research Institute for Earth Science and Disaster Resilience. This study was supported by the Japan Society for the Promotion of Science, KAKENHI Grant 17K14724. We also express our appreciation to two anonymous reviewers for their insightful comments.

Author contribution statement: WY and KI drafted the manuscript. WY analysed the SAR data, and WY, KI and TM interpreted the estimated surface displacement. MU interpreted the related resistivity structure. All the authors discussed the research and results and approved the final manuscript.

REFERENCES

Asano, K & Iwata, T, 2016. Source rupture processes of the foreshock and mainshock in the 2016 Kumamoto earthquake sequence estimated from the kinematic waveform inversion of strong motion data, *Earth Planets Space,* **68**(8):147, doi:10.1186/s40623-016-0519-9.

Aster, R.C., Borchers, B. & Thurber, C.H., 2013. *Parameter Estimation and Inverse Problems,* Elsevier.

Chen, C.W. & Zebker, H.A., 2000. Network approaches to two-dimensional phase unwrapping: intractability and two new algorithms, *J. Opt. Soc. Am. A,* **17,** 401–414.

Dieterich, J. H. & ,Decker, R. W., 1975, Modeling of surface deformation associated with volcanism, *J. Geophys. Res.,* **80,** 29, 4094–410.

Fialko, Y., 2004. Evidence of fluid-filled upper crust from observations of postseismic deformation due to the 1992 M_w 7.3 Landers earthquake, *J. geophys. Res.,* **109,** B08401, doi:10.1029/2004JB002985.

Fialko, Y, Simons, M & Khazan, Y, 2001. Finite source modelng of magmatic unrest in Socorro, New Mexico, and Long Valley, Callifornia, *Geophys. J. Int.,* **146**(8):191–200.

Hata, M., Takakura, S., Matsushima, N., Hashimoto, T. & Utsugi, M., 2016. Crustal magma pathway beneath Aso caldera inferred from 3-D electrical resistivity structure, *Geophys. Res. Lett.,* **43**(20), 10 720–10 727.

Hata, M., Matsushima, N., Takakura, S., Utsugi, M., Hashimoto, T. & Uyeshima, M., 2018. 3-D electrical resistivity modeling to elucidate the crustal magma supply system beneath Aso caldera, Japan, *J. geophys. Res.,* **123**(8), 6334–6346.

Hill, D.P., Pollitz, F. & Newhall, C., 2002. Earthquake−volcano interactions, *Phys. Today,* **55,** 41–47.

Himematsu, Y. & Furuya, M., 2016. Fault source model for the 2016 Kumamoto earthquake sequence based on ALOS-2/PALSAR-2 pixel-offset data: evidence for dynamic slip partitioning, *Earth Planets Space,* **68,** 169, doi:10.1186/s40623-016-0545-7.

Ishitsuka, K., Matsuoka, T., Nishimura, T., Tsuji, T. & ElGharbawi, T., 2017. Ground uplift related to permeability enhancement following the 2011 Tohoku earthquake in the Kanto plain, Japan, *Earth Planets Space,* **69,** 81, doi:10.1186/s40623-017-0666-7.

Japan Meteorological Agency (JMA), 2016. 'Seismic and volcanic activity on October 2016'. Available at: https://www.jma.go.jp/jma/press/1611/09a/1610jishin.pdf. (in Japanese) (Last view: 7th May 2019).

Jonsson, S., Segall, P., Pedersen, R. & Bjornsson, G., 2003. Post-earthquake ground movements correlated to pore-pressure transients, *Nature,* **424,** 179–183.

Kagabu, M., Ide, K., Hosono, T., Nakagawa, K. & Shimada, J., 2018. Numerical tank model analysis of coseismic groundwater-level increasing induced by 2016 Kumamoto earthquake, in *2018 JpGU Annual Meeting*, AHW24-P06.

Manga, M., Beresnev, I., Brodsky, E.E., Elkhoury, J.E., Elsworth, D., Ingebritsen, S.E., Mays, D.C. & Wang, C.-Y., 2012. Change in permeability caused by transient stresses: field observations, experiments, and mechanisms, *Rev. Geophys.,* **50,** RG2004, doi:10.1029/2011RG000382.

Massonnet, D. & Feigl, K.L., 1998. Radar interferometry and its application to changes in the Earth's surface, *Rev. Geophys.,* **36**(4), 441–500.

Masterlark, T., 2007. Magma intrusion and deformation predictions: sensitivities to the Mogi assumptions, *J. geophys. Res.,* **112,** B06419, doi:10.1029/2006JB004860.

Masterlark, T., Donovan, T., Feigl, K. L., Haney, M., Thurber, C. H. & Tung, S., 2016. Volcano deformation source parameters estimated from InSAR:

sensitivities to uncertainties in seismic tomography, *J. geophys. Res.,* **121,** 3002–3016.

Miyakawa, A., Sumita, T., Okubo, Y., Okuwaki, R., Otsubo, M., Uesawa, S. & Yagi, Y., 2016. Volcanic magma reservoir imaged as a low-density body beneath Aso volcano that terminated thr 2016 Kumamoto earthquake rupture, *Earth Planets Space,* **68,** 208, doi:10.1186/s40623-016-0582-2.

Mogi, K., 1958. Relations between the eruptions of various volcanoes and the deformation of the ground surfaces around them, *Bull. Earthq. Res. Inst.,* **36,** 99–134.

Nishiguchi, T., Tsuchiya, S. & Imaizumi, F., 2017. Detection and accuracy of landslide movement by InSAR analysis using PALSAR-2 data, *Landslides,* **14**(4), 1483–1490.

Nobile, A., Acocella, V., Ruch, J., Aoki, Y., Borgstrom, S., Siniscalchi, V. & Geshi, N., 2017. Steady subsidence of a repeatedly erupting caldera through InSAR observations: Aso, Japan, *Bull. Volcanol.,* **79,** 32, doi:10.1007/s00445-017-1112-1.

Ohzono, M., Ohta, Y., Iinuma, T., Miura, S. & Muto, J., 2012. Geodetic evidence of viscoelastic relaxation after the 2008 Iwate-Miyagi Nairiku earthquake, *Earth Planets Space,* **64**(9), 759–764.

Ozawa, T., Fujita, E. & Ueda, H., 2016. Crustal deformation associated with the 2016 Kumamoto earthquake and its effect on the magma system of Aso volcano, *Earth Planets Space,* **68,** 186, doi:10.1186/s40623-016-0563-5.

Peltzer, G., Rosen, P., Rogez, F. & Hudnut, K., 1998. Poroelastic rebound along the Landers 1992 earthquake surface rupture, *J. geophys. Res.,* **103,** 30 131–30 145.

Reinsch, T., Dobson, P., Asanuma, H., Huenges, E., Poletto, F. & Sanjuan, B., 2017. Utilizing supercritical geothermal systems: a review of past ventures and ongoing research activities, *Geotherm. Energy,* **5,** 16, doi:10.1186/s40517-017-0075-y.

Sudo, Y. & Kong, L.S.L., 2001. 3-D seismic velocity structure beneath Aso volcano, Kyushu, Japan, *Bull. Volcanol.,* **63,** 326–344.

Sudo, Y., Tsutsui, T., Nakaboh, M., Yoshikawa, M., Yoshikawa, S. & Inoue, H., 2006. Ground deformation and magma reservoir at Aso volcano: location of deflation source derived from long-term geodetic surveys, *Bull. Volcanol. Soc. Japan,* **51,** 291–309.

Takada, Y. & Fukushima, Y., 2013. Volcanic subsidence triggered by the 2011 Tohoku earthquake in Japan, *Nat. Geosci.,* **6,** 637–649.

Wang, C-Y., Wang, C-H. & Manga, M., 2004. Coseismic release of water from mountains: evidence from the 1999 ($M_w = 7.5$) Chi-Chi, Taiwan, earthquake, *Geology,* **32,** 769–772.

Yagi, Y., Okuwaki, R., Enescu, B., Kasahara, A., Miyakawa, A. & Otsubo, M., 2016. Rupture process of the 2016 Kumamoto earthquake in relation with the thermal structure around Aso volcano, *Earth Planets Space,* **68**(1), 1–6.